

Beam Injection Flame Furnace Atomic Absorption Spectrometry: A New Flame Method

Attila Gáspár and Harald Berndt*

Institut für Spektrochemie und angewandte Spektroskopie, Bunsen-Kirchhoff-Strasse 11, 44139 Dortmund, Germany

A new flame method of atomic absorption spectrometry is described. The liquid sample to be analyzed is transported as a high-speed liquid jet into a heated tube which is positioned in an air/acetylene flame. The jet is generated by means of an HPLC pump which feeds a smooth jet nozzle having a diameter of 50 μm or smaller. After traveling a distance of 10 cm, the liquid jet enters a small sample introduction hole, impacts onto the opposite inner wall of the tube furnace, and immediately vaporizes (jet impact vaporization, JIV). Both the complete introduction of the entire sample and the extended residence time inside the absorption volume result in an improvement in power of detection from 6- to 202-fold for 17 elements (Ag, As, Au, Bi, Cd, Cu, Hg, In, K, Pb, Pd, Rb, Sb, Se, Te, Tl, Zn). A standard deviation of 1.7–4.0% ($n = 12$, 50 μL) was achieved. Sample volumes between 10 μL and 1 mL have been investigated. For 50 μL sample volumes, the sampling frequency is 4/min. The new method can also be considered a simple, effective interface between HPLC and flame AAS.

The detection power of flame atomic absorption spectrometry can be improved by increasing the efficiency of aerosol generation/transport and prolonging the residence time of the free analyte atoms in the absorption volume. Ideal liquid sample introduction implies a reproducible transfer of the total sample solution into the atomization cell. The direct introduction of the entire sample into the flame without nebulization can be performed by the boat-in-flame technique¹ and the Delves cup technique.² Delves introduced a nickel microcrucible into the flame, above which a nickel absorption tube was positioned. As the sample vaporized, it was transported through a hole, together with some flame gases, and was collected in the nickel tube. Since the temperature inside the cup and the tube was less than the flame temperature, these techniques were only effective for elements which are relatively volatile (Ag, As, Bi, Cd, Hg, Pb, Se, Te, Tl, Zn).³ From a different point of view, the nickel tube can be considered as a flame-heated tube furnace in which a gaseous sample is introduced. The widest application of flame-heated tube furnaces involves the determination of hydride-forming elements, whereby the gaseous hydrides are introduced into a hot T-shaped

quartz tube (HG-AAS). The simplest way to increase the residence time of the analyte in the flame is through the use of a slotted quartz tube ("atom trap") placed in the flame. Due to the slight prolongation of the residence time of the flame gases in the absorption volume, the improvement factor for measurements is only 1.1–5 for easily volatilized elements.³ A review by Matusiewicz gives a detailed description of the various possibilities for improving the power of detection of flame AAS with atom-trapping techniques.⁴

The possibility of introducing not only gaseous components but also liquids directly into a heated tube positioned in the flame has already been demonstrated in the first paper on hydraulic high-pressure nebulization (HHPN).⁵ A fine and very narrow aerosol beam, generated at about 200 bar by means of a 20 μm plane orifice nebulizer, was directed through a sample introduction hole into a ceramic tube positioned in the flame. This led to a 20-fold increased power of detection for the determination of lead.⁵ Use of a suitable smooth jet nozzle instead of the highly turbulent HHPN nozzle permits generation of a high-speed liquid beam in a simple way even with a very low back-pressure. Due to the very small flow rates needed for atomic spectrometry, nozzles with openings of 50 μm or smaller are required.

This paper describes the disintegration of a high-speed liquid jet inside a flame heated tube furnace. The furnace can be made of different metals, alloys, or ceramics. The sample to be nebulized, vaporized, and atomized is introduced as a free-flying liquid beam through a sample introduction hole where it impacts on the inner surface of the heated tube. The distance between the nozzle and the furnace is about 10 cm. The kinetic energy of the jet must be high enough to guarantee flight stability, thereby permitting the jet to enter a small sample introduction hole with good reproducibility even after this rather long flight distance. The droplets originally generated by the impact of a 50 μm liquid beam onto the heated wall are vaporized spontaneously in the very hot environment inside the tube furnace. A pure jet impact nebulization (JIN) for sample introduction has already been used with flame photometry⁶ and successfully applied for sample introduction in ICP/AES.⁷ In both cases, the aerosol is produced in a nebulizer chamber and then transported by a carrier gas into a flame⁶ or plasma.⁷ The new combined mechanism of jet impact nebulization and spontaneous vaporization is termed jet impact

(1) Kahn, H. L.; Peterson, G. E.; Schallis, J. E. *At. Absorpt. Newsl.* **1968**, 7, 35–39.

(2) Delves, H. T. *Analyst* **1970**, 95, 431–438.

(3) Welz, B.; Sperling, M. *Atomabsorptionsspektrometrie*, 4th ed.; Wiley-VCH: Weinheim, Germany, 1997; p 28 (ISBN 3-527-28305-6).

(4) Matusiewicz, H. *Spectrochim. Acta* **1997**, 52B, 1711–1736.

(5) Berndt, H. *Fresenius' J. Anal. Chem.* **1988**, 331, 321–323.

(6) Hermann, R.; Alkemade, C. Th. J. *Flammenphotometrie*, 2nd ed.; Springer: Berlin, 1960; pp 92–93.

(7) Doherty, M. P.; Hieftje, G. M. *Appl. Spectrosc.* **1984**, 38, 405–412.

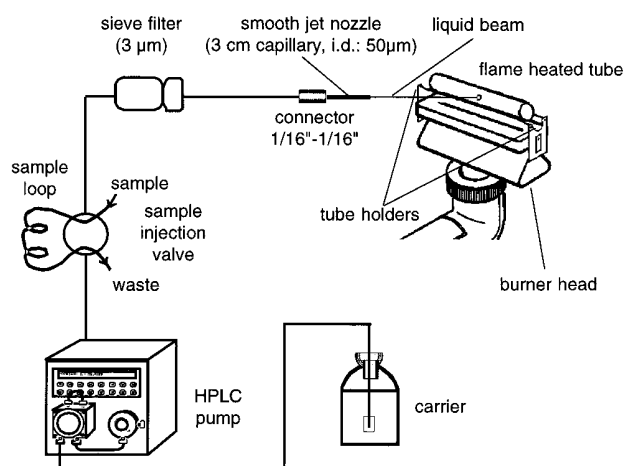


Figure 1. Schematic arrangement of the BIFF-AAS system.

vaporization (JIV). The total sample is transported to the absorption volume, and as in all other heated-tube techniques (furnace techniques), a relatively long residence time of the sample is also obtained. Due to both factors, a significant improvement in the power of detection can be expected for a number of elements.

The system described in this paper consists of a flame-heated tube furnace (flame furnace) and a liquid beam generation/sample introduction unit. This method is termed beam injection flame furnace AAS (BIFF-AAS). In this study, the basic investigations, optimization, and evaluation of BIFF-AAS are described. The characteristics of 17 high- or medium-volatility elements determined by BIFF-AAS are presented. Different arrangements and tube materials (flame furnaces) as well as some possible interferences are investigated and discussed.

EXPERIMENTAL SECTION

Standard Instrumentation. *Spectrometer.* A Varian model 1475 double-beam flame atomic absorption spectrometer equipped with deuterium lamp background correction was used. Operating parameters (wavelength, slit, current for the hollow cathode lamp) for the spectrometer were as recommended by the manufacturer. In all experiments, an acetylene/air flame was used.

Data Evaluation. A 486 PC fitted with an HPLC software–hardware combination (version 2.2; Knauer) was interfaced to the analog output of the spectrometer, and an additional interface/relay box permitted automatic operation of the HPLC. In some cases, for better illustration of the original signals, data were transferred to a spreadsheet program.

Sample Introduction/Beam Generation. A standard HPLC pump (Knauer), a six-port sample injection valve (PEEK, polyether ether ketone), a 3 μm titanium sieve protection filter, a PEEKsil capillary (i.d. 50 μm) (Scientific Glass Engineering) and PEEK tubing (0.17 mm i.d.) were used throughout.

Arrangement of the BIFF-AAS System. The schematic setup of the BIFF-AAS system is shown in Figure 1. The transport of the liquid and sample injection are similar to those for HPLC using an HPLC pump, a six-port sample injection valve, different sample loops (10 μL –1 mL), PEEK tubing, and a protective sieve filter. The necessary minimal back-pressure for running the HPLC pump (some hundred kilopascals) is provided by the flow resistance of the nozzle. As a convenient and inexpensive nozzle, a short piece

of a gas chromatographic capillary tube can be used. Such capillaries with 50 μm inner diameter are even available coated with PEEK or other polymers having an outer diameter of $1/16$ in. such that they can be connected to standard HPLC tubing and fittings. To keep the dispersion of the sample solution small, 0.17 mm inner diameter PEEK tubes are used and the lengths of the tubes are as short as possible. The capillary nozzle (3 cm length) is fixed with an adjustable holder in front of the flame furnace. The distance between the end of the PEEKsil capillary and the tube is about 10 cm. A distance within a range of 5–15 cm has no effect on the signal obtained. The optimal angle between the liquid beam and the impact surface inside the atomization tube is $\approx 90^\circ$. Small metal plates are attached (screwed) to both ends of the burner head onto which two ceramic pins of 3 cm length are fixed. The tube is placed on these pins and can be moved into/out of the flame easily. This arrangement makes it possible to position the tube in the flame over its full length without cold ends. The distance between the burner surface and the lower surface of the tube is about 10 mm.

Liquid Jet Generation and Introduction. For BIFF-AAS, it is necessary to generate a stable, linearly directed liquid beam, which can be aimed through a hole of 2 mm diameter into the heated tube. Additionally, the beam has to penetrate a perpendicular flow of high-velocity flame gases around the tube, to pass through the inner diameter of the tube, and to finally impact the hot inner surface of the tube while breaking through the layer of vapor formed due to the Leidenfrost phenomenon. The residence time of this beam in the hot tube (travel time between the entrance hole and the impact point) is only about 1 ms. During this short time, evaporation of the liquid beam is negligible due to the poor heat transfer between the liquid beam and the hot gaseous environment.

The most important factor both for the formation of a stable liquid beam and for the effective impact of the beam on a surface is the kinetic energy of the beam. The latter increases significantly with its speed ($E_{\text{kin}} \sim v^2$). Initial experiments showed that a beam was stable over a distance of at least 10 cm or more if the speed of the beam was higher than about 12 m/s. Using a nozzle of 50 μm inner diameter, a 1.42 mL/min flow rate is necessary to reach this required speed. The typical shape of a smooth jet nozzle is a cylinder with a ratio $L/d > 3$. The flow inside such nozzles can be considered laminar if the Reynolds number is smaller than 2200. The working pressure of this type of nozzle can be calculated using the Hagen–Poiseuille law. For a flow rate of 1.5 mL/min and a length of 1 cm, the pressure drop amounts to 1.6 MPa. The length of the capillary causes no difference in the properties of the liquid beam because the velocity is independent of the length if a constant flow rate is used.

It could be expected that increasing the flow rate would lead, on one hand, to improved nebulization due to the higher kinetic energy of the beam but, on the other hand, to a lower temperature inside the tube due to the high vaporization enthalpy of the vaporized water. The temperature (measured with thermocouples) inside the atomization tube was about 1050 $^\circ\text{C}$ (Ni tube with additional holes on the bottom side) without introducing water. With 1, 1.5, and 2.5 mL/min sample flow rates, the temperature decreased to 1010, 940, and 850 $^\circ\text{C}$, respectively. The effect of the sample flow rate on peak height and peak area for the

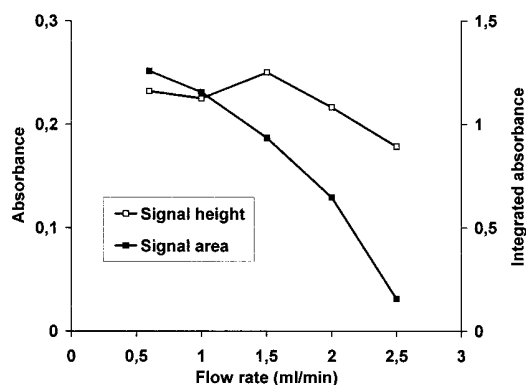


Figure 2. Influence of the liquid flow rate on the height and the area of the signals obtained for 50 μL samples of 0.5 $\mu\text{g/mL}$ Pb (Ni tube furnace with additional holes).

introduction of lead is shown in Figure 2. While the signal area decreases continuously with increasing flow rate, peak height increases to a maximum at about 1.5 mL/min. The decrease in the peak area can be explained by the lower temperature in the tube and the faster throughput of the small sample volume, whereby the width of the signal becomes smaller. The small maximum in peak height at about 1.5 mL/min is also noted with measurements of all other elements. A possible explanation may be the convoluted effects of a more effective nebulization due to the increasing flow rate and a lower atomization rate due to the lower temperature inside the tube caused by the larger amount of water vaporized. At flow rates of 1.5 mL/min or higher, a small, very sharp dark spot (smaller than 1 mm) can be seen on the inner heated wall of the tube opposite the entrance hole. This reflects the effective impact of the beam on the inner wall of the tube.

Material, Shape, and Working Conditions for the Flame Furnace. The requirements for the material of the tube include good stability and chemical resistance to the corrosive conditions of an acetylene/air flame. There are also high demands for chemical resistance against water and acid vapors at temperatures higher than 1000 °C. The following materials were investigated for their suitability: pure nickel tubes (12/10 mm o.d./i.d.), a certified superalloy (ASTM B 167: 74% Ni, 16% Cr, 9% Fe; 14/12, 12/10, 10/8, 8/6 mm o.d./i.d.), nonporous Al_2O_3 ceramic (>99.7%; Alsint, Haldenwanger, Germany; 8/5 mm o.d./i.d.), and quartz (16/13 mm o.d./i.d.). Initial experiments with a ceramic tube having a porous surface were undertaken because this material tolerates rapid and large temperature changes. However, serious memory effects due to the adsorption of analyte atoms on the porous inner surface arose. Clearly, the surface of the wall must be smooth and nonporous, e.g. Alsint ceramic. The lifetimes of the nickel and nickel alloy furnaces appear to be nearly unlimited. The lifetime of the ceramic atomization tubes in the flame was more than 100 h. However, after several hours, short, hairline cracks appeared around the sample introduction holes of these tubes, which caused subsequent breakage. Quartz furnaces with relatively thick walls (1.5 mm) were also stable for more than 100 h under the conditions of BIFF-AAS, but due to unsatisfactory analytical results, ceramic or metal tubes were preferred. One reason for the poorer performance of the quartz tubes could be connected with the heat conductivity of the quartz (glass: 0.6–

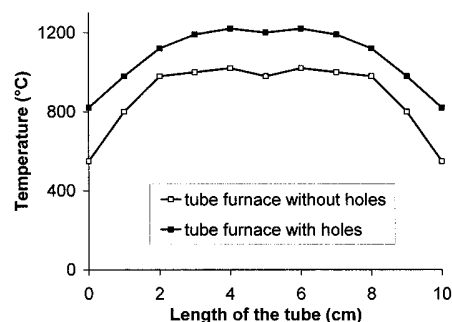


Figure 3. Temperature profiles of a tube (flame furnace) with additional holes and a tube without additional holes (ceramic tube; i.d., 6 mm; flow rate 1.5 mL/min).

1.0 $\text{W K}^{-1} \text{m}^{-1}$), which is considerably lower than that of Ni (52 $\text{W K}^{-1} \text{m}^{-1}$) or the ceramic (34 $\text{W K}^{-1} \text{m}^{-1}$). This means that, in the case of quartz, the upper part of the tube may have a considerably lower temperature than the lower part. The optimal inner diameter of the atomization tube lies between 6 and 10 mm; a larger tube leads to a lower temperature, and the sample residence time with a smaller tube becomes shorter due to the higher velocity of the vapor formed from the vaporized water (smaller volume of the tube). The length of the tube is limited to the length of the burner slot, and thus a tube of 100 mm length was used. With a liquid flow rate of 1.5 mL/min and a tube of 10 mm inner diameter (inner volume: 7.8 mL), the vapor flow rate amounts to 8700 mL/min at a temperature of 1000 °C. This means that the average residence time of the vapor inside the tube is 54 ms, which is more than 10 times longer than the residence time in an unobstructed AAS flame.

The 2 mm hole in the middle of the tube is large enough to introduce the very narrow liquid jet into the furnace yet small enough to keep the sample vapor in the tube. It can be assumed that no flame gases are entering the tube through the sample introduction hole because the plane of this hole is essentially parallel to the direction of flow of the flame gases. The lack of flame gases inside the atomization tube creates a significantly lower temperature than the flame temperature. Due to the low temperature, only highly volatile elements with low appearance temperatures (e.g., Hg and Cd) can be determined with satisfying results. To enhance the temperature and to achieve a more reducing atmosphere, a tube with four or more additional holes of 2 mm diameter located on the bottom side was used. The temperature distributions inside ceramic atomization tubes with and without holes are shown in Figure 3. The temperature in the tube containing these holes is about 200 °C higher than in the tube without holes. In the case of the tube with additional holes, the reported temperature should be regarded as relative because the higher real temperature (flame temperature) cannot be measured using thermocouples due to the small heat capacity of the flame gases.

Figure 4 shows signals from Hg and Zn using a furnace without and one with additional holes. In the case of Hg, the signals become smaller by about 15% using the furnace with holes because the additional flame gases dilute the sample vapor and also likely reduce the residence time in the furnace. In contrast to this result, the signal from Zn is considerably increased when the furnace with holes is used. Due to the higher appearance temperature of

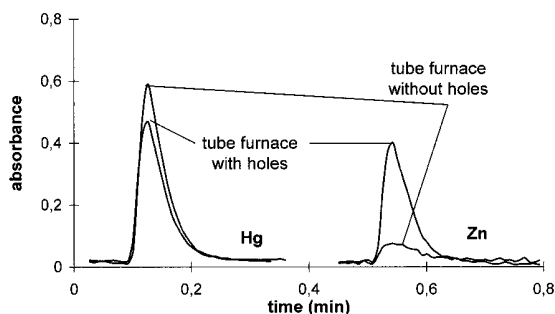


Figure 4. Comparison of the signals from 50 μL samples of Hg (20 $\mu\text{g/mL}$) and Zn (0.1 $\mu\text{g/mL}$) obtained by using tube furnaces with additional flame introduction holes and without additional holes (flow rate 1.5 mL/min).

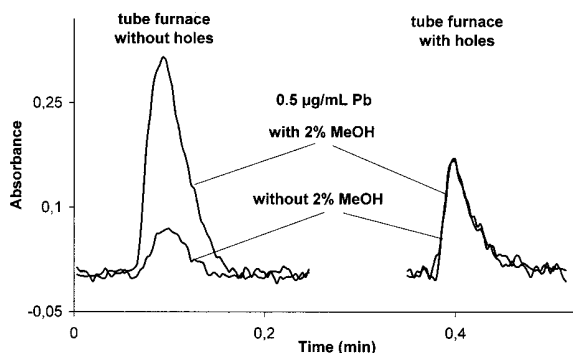


Figure 5. Influence of 2% methanol content in the sample on the signals obtained using a tube furnace with additional holes and a tube without additional holes (sample 50 μL ; 0.5 $\mu\text{g/mL}$ Pb; flow rate 1.5 mL/min).

Zn, the increase of sensitivity with temperature is much larger than the loss of sensitivity caused by dilution. When a furnace without holes is used, a significant increase in sensitivity can be achieved for some elements by adding a small amount of methanol to the sample solution. Figure 5 shows the influence of 2% methanol on the response from Pb in both furnace types. In the case of the furnace without additional holes ("closed furnace"), the signal area is increased approximately 5-fold using 2% methanol (Figure 5, left side). Using a furnace with additional holes ("open furnace") shows that it makes no difference whether the sample contains methanol or not (Figure 5, right side). Similar results were obtained for Zn and Tl. The dependence of signal intensity on methanol concentration in a "closed furnace" is shown in Figure 6. These data show that a small amount of methanol leads to a considerable improvement in sensitivity whereas a concentration higher than 2% only serves to enhance dilution, resulting in a lower sensitivity. The increase in sensitivity is probably due to a reducing atmosphere inside the furnace caused by the methanol. For mercury, the influence of methanol (Figure 7) is much smaller than that for Pb, Zn, and Tl. An explanation could be that the low appearance temperature of Hg already leads to maximum possible sensitivity achieved with a furnace without holes. This figure also shows a comparison with pneumatic nebulization (PN; conventional mode of flame AAS). Other organic solvents, e.g., acetonitrile, increase signals similarly to methanol, but a detailed study of this effect is beyond the framework of this paper. The composition of the acetylene/air flame has only a small

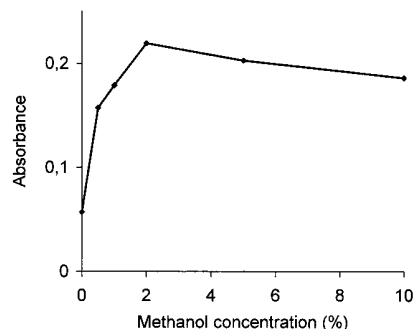


Figure 6. Influence of the methanol concentration in the sample on the signal height for the measurement of Pb in a tube furnace without additional holes (sample 50 μL ; 0.5 $\mu\text{g/mL}$ Pb; flow rate 1.5 mL/min).

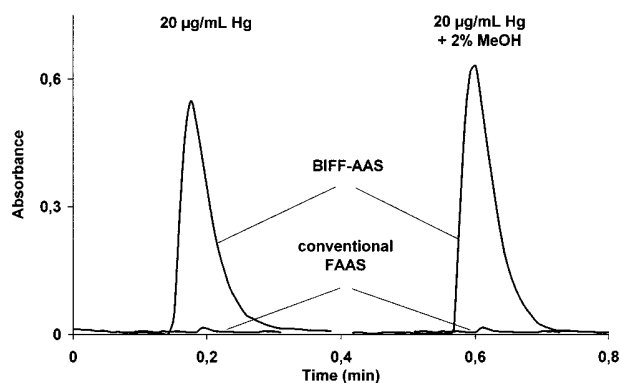


Figure 7. Influence of 2% methanol on the signal from a 50 μL sample of 20 $\mu\text{g/mL}$ Hg obtained by BIFF-AAS (Ni tube furnace without additional holes; flow rate 1.5 mL/min) and conventional FAAS.

influence on the atomization conditions inside the tube. For all elements studied, a fuel-lean or stoichiometric flame was appropriate.

It must be emphasized that the flame gases should not be ignited when the tube containing holes along the bottom has been placed on the burner head because the tube may become filled with an explosive mixture of acetylene/air during ignition of the flame. To avoid a dangerous explosion, the atomization tube should only be placed onto the burner head after ignition of the flame.

RESULTS

Currently, 25 elements have been determined using BIFF-AAS, of which 17 elements (Ag, As, Au, Bi, Cd, Cu, Hg, In, K, Pb, Pd, Rb, Sb, Se, Te, Tl, Zn) exhibit a better power of detection compared to that of conventional FAAS.

Sample Amount. With BIFF-AAS, the sample is introduced into a carrier stream, as in all flow injection techniques and HPLC, which results in transient signals. The use of a standard HPLC pump for the pressure generation also permits the use of low dead volume HPLC equipment such as valves, connection tubing, and filters, which keep the dilution (dispersion) of the sample small. Therefore, even sample volumes as small as 10 μL can be easily handled. Figure 8 shows the signals for 10, 50, 100, and 200 μL of a 0.2 $\mu\text{g/mL}$ solution of Cu. For these measurements, a ceramic tube (6 mm i.d.) with four holes along the bottom was used. For

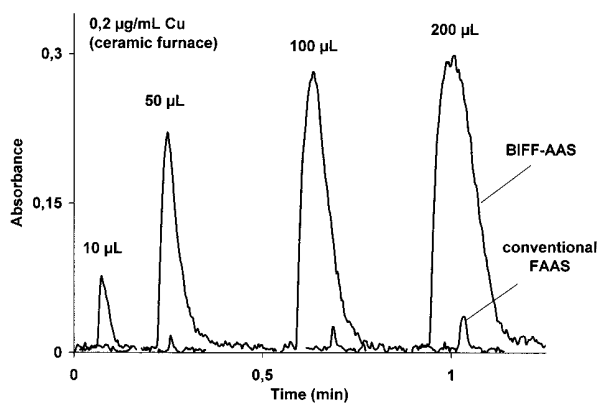


Figure 8. Signals from 0.2 $\mu\text{g/mL}$ Cu samples of different volumes (10, 50, 100, and 200 μL) obtained by BIFF-AAS (ceramic tube furnace with additional holes; i.d. 6 mm; flow rate 1.5 mL/min) and conventional FAAS.

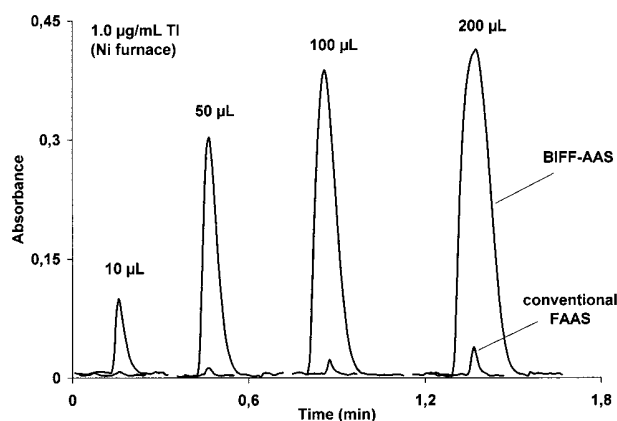


Figure 9. Signals from 1.0 $\mu\text{g/mL}$ Tl samples of different volumes (10, 50, 100, and 200 μL) obtained with BIFF-AAS (Ni tube furnace with additional holes; i.d. 10 mm; flow rate 1.5 mL/min) and conventional FAAS.

a flow rate of 1.5 mL/min, the maximum signal intensity was achieved with a sample volume of 100 μL . The same trend was observed with all other elements, even with different furnaces. Figure 9 shows data for the introduction of a 1 $\mu\text{g/mL}$ sample of Tl into a nickel furnace (10 mm i.d.) with holes. The better signal-to-noise ratio for Tl compared to Cu may be the result of the different size and materials of the furnace (more investigations are necessary). In both figures, the signals obtained using pneumatic nebulization with discrete sample injection are also shown. Both the signal height and area considerably increased when BIFF-AAS instead of the standard working mode of FAAS was used. Even for a sample volume of only 10 μL , concentrations of 0.2 $\mu\text{g/mL}$ Cu and 1 $\mu\text{g/mL}$ Tl can be measured, which is not possible with standard FAAS.

Comparison of BIFF-AAS and Conventional FAAS. Due to the large number of measurements, this comparison was only done with 50 μL sample volumes. For all 25 elements investigated, single-element solutions containing 0.1 M HNO_3 were prepared and the standard deviation of each was determined by following 12 replicate measurements. All data acquisition was done with HPLC software. The original spectrometer had no built-in screen, but with a separate PC and HPLC software, all signals could be visualized, recorded, and stored. The software also permitted

transfer of the raw data to other PC programs. Detection limits were calculated on the basis of 25 measurements of the blanks (carrier).

Table 1 presents the statistical data for the measurements of both signal height and area. The improvement in power of detection is best using signal area. Improvements of about 200-fold were found for Hg and Cd using a flame furnace without additional holes. A 100-fold improvement in the power of detection was achieved for lead. The improvement factor between BIFF-AAS and conventional FAAS varies from 6- to 202-fold for signal area and from 1.5- to 69-fold for signal height, depending on the element. The relative standard deviations amount to 1.7–4.0% for signal area and 2.0–4.5% for signal height. The sampling frequency is 4/min for 50 μL sample volumes. In contrast to the case of the 17 elements mentioned above and listed in Table 1, the sensitivity for Na, Li, Mg, Mn, Cr, Fe, Co, and Ni was lower than that for conventional flame AAS (depending on the element, by a factor of 0.2–0.8). Therefore, this group of elements was not further investigated.

Larger sample volumes lead to an improved signal-to-noise ratio for BIFF-AAS and conventional flame AAS. Improvement factors for both methods will not increase by applying, for instance, 1 mL of sample instead of 50 μL of sample, but the detection limit for BIFF-AAS will be lowered. This was only studied for one element (Pb), for which the detection limit was improved 4-fold by increasing the sample volume 20-fold (50 $\mu\text{L}/1\text{ mL}$).

Matrix Effects. Only a few experiments have been conducted to obtain an estimate of the influence of matrix on response. Figure 10 shows results for the introduction of 0.10 $\mu\text{g/mL}$ Cu in the presence of 1, 5, and 10% (w/w) NaCl. The reason for the (unexpected) relatively low interference may be that the measurements were done with a tube furnace containing additional holes, whereby some of the flame gases enter the tube, thereby raising the temperature inside the tube sufficiently to ensure the total vaporization and dissociation of the NaCl particles. Further systematic studies concerning matrix interference are necessary.

DISCUSSION

Beam injection flame furnace AAS is characterized by sample introduction via a horizontal liquid beam passing into a hot tube positioned in the AAS flame. Using such a flying beam, the total sample is transported directly to the vaporization/atomization cell. In addition to total sample introduction, a long residence time accrues for the atomized elements in the absorption volume. These two effects lead to a considerable improvement in the power of detection for high- and medium-volatility elements. For the first time, a very hot surface, i.e., the inner wall of the flame-heated tube, is used for jet impact nebulization. In BIFF-AAS, jet impact nebulization is directly combined with the vaporization of the aerosol due to the extremely hot environment (jet impact vaporization, JIV). In the case of impact nebulization on a hot surface, additional effects caused by the Leidenfrost phenomenon must also be considered. As a result of this phenomenon, formation of a thermally insulating vapor occurs at the moment of liquid impact on the wall. This should be avoided for effective jet impact nebulization. To break through this vapor layer and to contact the hot wall (about 1000 $^{\circ}\text{C}$), a liquid beam with high velocity (high kinetic energy) is necessary. Since the temperature of the tube lies far above the Leidenfrost point, droplets formed

Table 1. Statistical Data (Standard Deviations ($n = 12$)) and Detection Limits ($n = 25$; 3σ Values) for 17 Elements Using Beam Injection Flame Furnace AAS and a Comparison of the Detection Limits for BIFF-AAS and Conventional FAAS

		signal height				signal area			
		RSD (%)	detection limit (ng/mL)		improvement of power of detection	RSD (%)	detection limit (ng/mL)		improvement of power of detection
concn ($\mu\text{g/mL}$)			BIFF-AAS	PN			BIFF-AAS	PN	
Cd ^a	0.1	2.3	0.25	17	69	1.7	0.078	15	193
Hg ^a	1	2.0	67	3600	54	2.1	19	3900	202
Ag	0.1	2.7	1.7	9.6	6	2.2	0.22	9.4	43
As	20	3.7	1000	1400	1.5	2.8	220	1300	6
Au	0.5	2.6	13	110	8	3.1	4.8	170	35
Bi	1	3.1	120	580	5	3.2	24	1100	47
Cu	0.2	2.3	1.4	31	22	2.2	0.44	28	64
In	1	3.8	110	310	3	3.7	30	310	10
K	0.2	2.8	1.7	6.9	4	2.9	0.26	7.9	31
Pb	0.5	2.4	25	660	26	2.4	6.8	690	101
Pd	1	2.8	55	560	10	2.5	14	570	40
Rb	1	4.2	23	83	4	3.9	4.7	100	22
Sb	1	4.0	49	740	15	3.9	12	690	57
Se	20	2.7	110	2000	18	3.3	23	1700	75
Te	1	4.5	47	690	15	4.0	9.6	660	69
Tl	0.5	3.3	6.9	160	23	2.4	2.1	150	71
Zn	0.1	2.2	0.4	9.6	24	1.9	0.13	12	92

^a Using a tube furnace without additional holes.

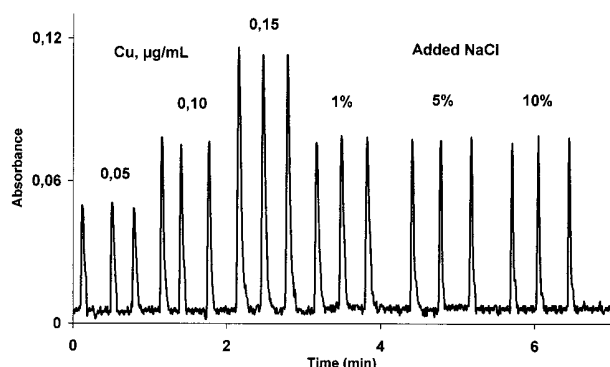


Figure 10. Signals from pure Cu solutions with increasing concentrations (0.05, 0.10, and 0.15 $\mu\text{g/mL}$) and from 0.10 $\mu\text{g/mL}$ Cu solutions in the presence of 1, 5, and 10% (w/w) NaCl (ceramic tube furnace with additional holes; sample 50 μL ; flow rate 1.5 mL/min).

during the initial impact are reflected by the wall and cannot become deposited. This is likely the reason for the minimal (nonobserved) memory effects. Only when porous ceramics are used as the furnace material are strong memory effects observed, probably because the analyte vapor penetrates the tube wall.

For JIN at room temperature, the optimal velocity required to convert the analyte solution to a spectroscopically useful aerosol was found to be 28–33 m/s.⁷ With flame-heated furnaces, the minimal velocity amounts to only 12 m/s. Using this velocity at room temperature, only a water drop is formed at the impact point, but no aerosol. This observation agrees with the description of JIN.⁷ In contrast to JIN, no liquid film or droplets can exist with JIV at the hot impact point. A part of the liquid beam will probably be vaporized just at this point. This vapor generation can also participate in the disintegration of the liquid jet. Currently, the details of this mechanism of JIV are unknown.

With BIFF-AAS, analytical signals decrease with an increased sample flow rate. If the tube furnace is fed with a higher sample flow rate, the vaporization rate becomes proportionally higher as

well. If all the water injected is vaporized, the average amount of sample inside the absorption volume will be independent of the sample flow rate. Finally, a high flow rate will only undesirably lower the temperature inside the tube. Therefore, small flow rates are preferable to higher flow rates for suitable analytical signals. Nevertheless, a flow rate of 1.5 mL/min is necessary because of the required kinetic energy of the liquid beam.

The quantity of heat needed to maintain the temperature of the furnace tube at 900 °C can be estimated from blackbody radiation considerations. For a tube with an outer diameter of 12 mm and a length of 100 mm, the calculated value amounts to 405 W. This means that the flame must transfer this amount of power to the tube furnace to compensate for the losses caused by blackbody radiation from the tube. Because blackbody radiation rapidly increases with temperature ($N \sim T^4$), the power must be increased from 405 to 760 W for an increase in wall temperature from 900 to 1100 °C. The practical attainable temperature of the furnace lies between 900 and 1000 °C, depending on its dimensions. Because of this relatively low temperature, only elements having a low appearance temperature (Hg, Cd) are easily determinable. The number of determinable elements increases to 25 if a tube furnace with additional holes along its bottom surface is used. In this case, a fraction of the flame gases enters the tube, whereby the temperature inside the tube is increased to values considerably higher than the wall temperature. Conclusions regarding an optimal arrangement of these holes and the true temperature inside the furnace cannot be drawn at this time, nor is the ratio of water vapor to flame gases inside the tube known.

CONCLUSION AND OUTLOOK

The flame is still the most frequently used atomizer in atomic absorption spectrometry,⁴ having the main advantages of simplicity, low interference, and high sample throughput. The new beam injection flame furnace AAS methodology serves to improve flame

techniques. With BIFF-AAS, a larger number of elements can be determined with higher sensitivity than with conventional flame AAS, but the level of detection of the graphite-furnace AAS technique is not achieved. Although mercury can be measured relatively sensitively with this flame method, if very low concentrations are to be determined, the cold vapor technique remains the better choice. For the first time, continuous liquid sample introduction into a tube furnace has become possible by means of a flying liquid beam. Using this technique, it is possible to introduce the sample from a distance of 10 cm into a heated metal or ceramic furnace. The improvement in the power of detection compared with that of standard flame AAS can also be of benefit for speciation analysis if the liquid jet is generated by an HPLC pump (interface-free coupling of HPLC techniques). Earlier applications of on-line preconcentration and matrix separation achieved with HHPN sample introduction can also be transferred to BIFF-AAS, including the full automation of this technique. As a sample loop is used, it is possible to work with BIFF-AAS using very small sample volumes, important for trace-element determinations in biological samples. All in all, hardware necessary for BIFF-AAS is relatively simple, consisting of a tube placed in the AAS flame, a pump and capillary to generate the liquid beam, and a sample introduction valve. Preliminary work shows that a pressure between 0.05 and 1 MPa, depending on the nozzle type, is sufficient such that the technique can be implemented with a low-pressure pump or even with a peristaltic pump (already

tested). Future investigations with smaller nozzles and lower flow rates (<0.5 mL/min) are planned to achieve higher temperatures inside the furnace. Further improvements may be expected if sample mixtures containing organic solvents are used instead of pure water beams. Due to a number of unresolved questions concerning the mechanism of jet impact vaporization and BIFF-AAS in general, a number of additional investigations are required, and in light of this, the present study has only served to provide preliminary information about this new flame AAS methodology.

ACKNOWLEDGMENT

This paper is dedicated to Prof. Dr. Klockow on the occasion of his 65th birthday. Our work was funded by the Bundesministerium für Bildung, Wissenschaft, Forschung und Technologie und dem Ministerium für Schule und Weiterbildung, Forschung und Technologie des Landes Nordrhein-Westfalen. Additional funds were supplied by the German Academic Exchange Service (Deutscher Akademischer Austauschdienst, DAAD) for the scholarship of A.G. at the Institut für Spektrochemie und angewandte Spektroskopie, Dortmund. Instrumental support was supplied by Varian.

Received for review April 5, 1999. Accepted October 10, 1999.

AC990342R